Bandgap and band offsets determination of semiconductor heterostructures using three-terminal ballistic carrier spectroscopy

Wei Yi,[1,a)] Venkatesh Narayanamurti,[1] Hong Lu,[2] Michael A. Scarpulla,[2] Arthur C. Gossard,[2] Yong Huang,[3] Jae-Hyun Ryou,[3] and Russell D. Dupuis[3]
[1]*School of Engineering and Applied Sciences, Harvard University, Cambridge, Massachusetts 02138, USA*
[2]*Department of Materials, University of California, Santa Barbara, California 93106, USA*
[3]*Center for Compound Semiconductors and School of Electrical and Computer Engineering, Georgia Institute of Technology, Atlanta, Georgia 30332, USA*

(Received 1 June 2009; accepted 20 August 2009; published online 14 September 2009)

Utilizing ambipolar tunnel emission of ballistic electrons and holes, we have developed a model-independent method to self-consistently measure bandgaps of semiconductors and band offsets at semiconductor heterojunctions. Lattice-matched GaAs/$Al_xGa_{1-x}As$ and GaAs/$(Al_xGa_{1-x})_{0.51}In_{0.49}P$ (100) single-barrier heterostructures are studied at 4.2 K. For the GaAs/AlGaAs interface, the measured Γ band offset ratio is 60.4:39.6 (±2%). For the heteroanion GaAs/AlGaInP (100) interface, this ratio varies with the Al composition and is distributed more in the valence band. The indirect-gap *X* band offsets observed at the GaAs/AlGaInP interface deviates from predictions by the transitivity rule. © *2009 American Institute of Physics*.
[doi:10.1063/1.3224914]

Among the most important properties of semiconductors are their bandgaps and how the total bandgap difference distributes between the conduction band offset ΔE_C and the valence band offset ΔE_V at the heterojunction (HJ) interface between two semiconductors. Understanding such properties is crucial for the design of HJ devices.

Traditionally, bandgaps are measured mostly with optical spectroscopies such as absorption and photoluminescence (PL).[1] Band offsets are measured electrically by thermionic emission and *C-V* profiling, optically by absorption and PL, and optoelectrically by photoelectron spectroscopies. However, each of these methods has certain limitations.[2] With a transistor setup, ballistic electron/hole emission spectroscopy (BEES/BHES) utilize ballistic injection of electrons/holes to probe the band offsets of HJs underneath a metal-semiconductor (m-s) interface.[3] However, to obtain the genuine barrier heights, a delta doping is needed to reach a flat-band condition across the HJ, which introduces a source of error due to the doping level.[4] Most of the aforementioned methods require separately designed *n*-type and *p*-type HJs to measure ΔE_C and ΔE_V independently, therefore, the results are not necessarily self-consistent.

In this letter, we report that the bandgap E_g of a semiconductor, as well as both ΔE_C and ΔE_V at a semiconductor HJ, can be measured on the same device. In contrast with previous BEES studies, our method utilizes selective injection of electrons and holes into the same m-s interface, realized by a collector bias V_C, which tunes the electric field (*E*-field) in the depletion region.[5] This enables measurement of the energy maxima in both the conduction band (CB) and the valence band (VB) of the HJ collector. Summing these two values gives the E_g of the corresponding constituent layer. An advantage of our method over optical spectroscopies is the absence of the generation and recombination of electron-hole pairs, therefore, it is free of exciton effects. In our previous report,[5] however, only one material ($Al_{0.4}Ga_{0.6}As$) was studied, therefore, band offset information was not obtained. Here we demonstrate that this method allows a precise measurement of ΔE_C and ΔE_V of a buried HJ over a wide range of constituent compositions.

As a proof of concept, ternary AlGaAs and quaternary AlGaInP III-V alloys are studied. Lattice-matched GaAs/AlGaAs and GaAs/AlGaInP single-barrier (SB) HJs are epitaxially grown on Zn-doped *p*-GaAs (100) substrates. After growing a 500 nm *p*-doped (5×10^{18} cm^{-3}) GaAs buffer layer (layer "4" in Fig. 1, and so forth), the unintentionally doped SB HJ is formed, with a 45 nm GaAs layer ("3"), a 50 nm AlGaAs or AlGaInP barrier layer ("2"), and a 5 nm GaAs cap layer ("1") for surface passivation. Samples with Al mole fraction x=0.0, 0.1, 0.2, 0.3, 0.42, 0.6, 0.8, and 1.0 for $Al_xGa_{1-x}As$, and x=0.0, 0.2, 0.35, 0.5, 0.7, 0.85, and 1.0 for $(Al_xGa_{1-x})_{0.51}In_{0.49}P$ are grown under exactly the same condition for each alloy system. Monolithic metal-base transis-

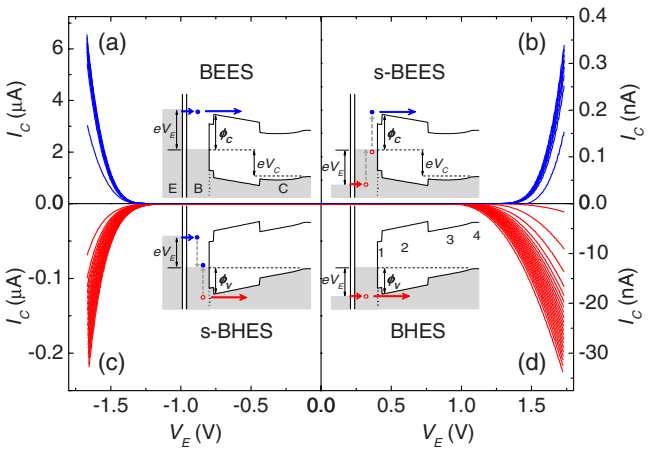

FIG. 1. (Color online) Band diagrams (insets) and collector-current (I_C) spectra of $Al_{0.42}Ga_{0.58}As$ sample taken at 4.2 K illustrating the direct and secondary BEES/BHES processes. Letter "E," "B," and "C" stand for emitter, base, and collector, respectively. Emitter current $I_E \approx 0.8(0.4)$ mA at $V_E = \mp 1.7$ V, and the flat-band $V_C \approx 0.5$ V for this particular device.

a)Electronic mail: weiyi@seas.harvard.edu.

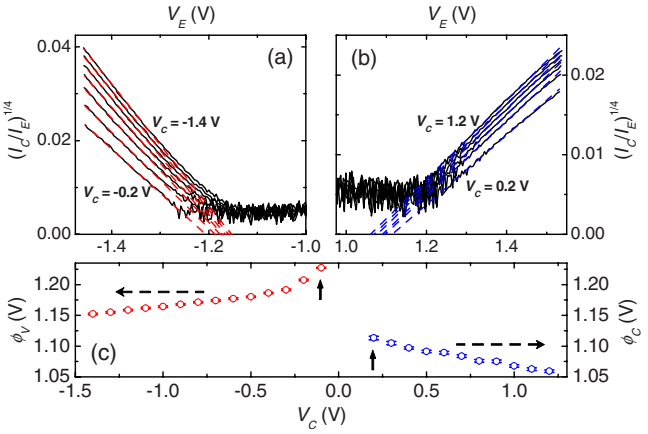

FIG. 2. (Color online) s-BHES/s-BEES of $(Al_{0.7}Ga_{0.3})_{0.51}In_{0.49}P$ sample taken at 4.2 K plotted as $(I_C/I_E)^{1/4}$ under negative (a) and positive (b) V_E superimposed with linear fits (dashed lines). The spectra are spaced at 0.2 V V_C intervals for clarity. (c) The measured ϕ_V and ϕ_C as a function of V_C. Vertical arrows show the values used to determine the E_g and band offsets.

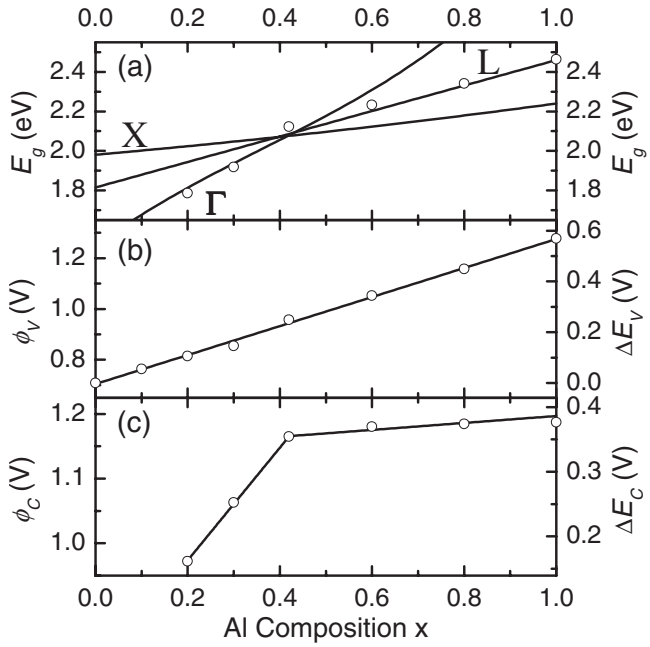

FIG. 3. Al composition x dependence of (a) E_g of $Al_xGa_{1-x}As$ (solid lines are from Ref. 7), (b) ϕ_V and ΔE_V of GaAs/$Al_xGa_{1-x}As$ (solid line is a linear fit), and (c) ϕ_C and ΔE_C of GaAs/$Al_xGa_{1-x}As$ (solid lines are linear fits).

tors, using planar Al/AlO_x/Al tunnel junctions as the tunnel emitters, are fabricated using a shadow-mask technique. The GaAs surfaces were treated in a 1:10 solution of $NH_4OH:H_2O$ for 60 s prior to Al evaporation. All the devices were characterized at 4.2 K to suppress the thermally excited currents.

Ambipolar carrier injection is made possible using BEES/BHES and their secondary/reverse processes (s-BEES/s-BHES) (Fig. 1). For example, in a s-BHES process, hot electrons tunnel into the base from a negatively biased emitter ($V_E<0$) with the p-type collector unbiased or in reverse bias [Fig. 1(c)]. The repulsive E-field in the CB prevents them from being collected across the m-s interface. Rather, they excite electron-hole pairs in the metal base in an Auger-like process. As a result, hot holes are produced and some of them may be ballistically injected into the VB of the collector and probe the VB barrier height ϕ_V. Under a forward V_C, the E-field in the CB becomes attractive to collect hot electrons injected by the direct BEES process, and the CB barrier height ϕ_C is probed [Fig. 1(a)]. Similar mechanisms apply for positive V_E [Figs. 1(b) and 1(d)]. E_g of the barrier layer is hence determined by summing these two barriers. The energy resolution of s-BEES is arguably superior to that of BEES owing to the quartic spectral shape of the two-step Auger process, i.e., near the threshold, the collector transfer ratio $\alpha \equiv I_C/I_E \propto (eV_E - \phi_{V(C)})^4$,[6] versus $\alpha \propto (eV_E - \phi_{V(C)})^2$ for BEES. Shown in Figs. 2(a) and 2(b), we found that a linear fit of $\alpha^{1/4} = \alpha_0(eV_E - \phi_{V(C)})$, with only two free parameters, gives $\phi_{V(C)}$ with a typical resolution ~2 meV at 4.2 K ($k_BT \sim 0.4$ meV), compared with ~20 meV resolution in typical BEES fitted by a multi-valley Bell–Kaiser model. The present fitting process does not require band parameters, e.g., effective masses, making it model independent. Note that the measured apparent barrier heights are subject to an image force lowering effect due to the E-field across the HJ. Therefore a series of BEES/s-BEES spectra are measured under constant V_C at small intervals (0.1 V or less). The measured barrier heights indeed depend on V_C [Fig. 2(c)]. ϕ_V and ϕ_C near the flat-band condition, where the transition from hole to electron injection occurs (telling from the polarity reversal of I_C), are used to calculate the E_g and band offsets.

The main results from the ternary AlGaAs alloy are shown in Fig. 3. The measured ϕ_V and ϕ_C as functions of Al composition x are shown in Figs. 3(b) and 3(c), respectively. ϕ_V increases linearly with x in the full range of Al composition ($0<x<1$), which is expected because all the VB maxima of AlGaAs are located at the Brillouin zone center. $\Delta E_V(x)$ of GaAs/$Al_xGa_{1-x}As$ is obtained by $\Delta E_V(x) = \phi_V(x) - \phi_V(0)$, where $\phi_V(0)$ is the value for GaAs. Here it is assumed that the Fermi level pinning position at the m-s interface (with regard to the vacuum level) remains unchanged for devices with different Al compositions, as supported by the fact that the measured ϕ_V shows a nearly perfect linear dependence on x. A linear fit gives $\Delta E_V(x) = (0.57 \pm 0.01)x$ (eV). $\Delta E_C(x)$ of GaAs/$Al_xGa_{1-x}As$ is derived from $\Delta E_C(x) = \phi_C(x) - E_g(0) + \phi_V(0)$, where $E_g(0)$ is the value for GaAs (taken as 1.519 eV at 4.2 K[7]). The derived $\Delta E_C(x)$ increases linearly with x in the direct regime, i.e., $\Delta E_C(x) = (0.87 \pm 0.01)x$ (eV) for $x<0.42$. A direct-indirect transition of the CB minima at $x=0.42$ is indicated by the abrupt slope change at this composition. In the indirect-gap regime, $\Delta E_C(x)$ slowly increases with x. The direct-gap Γ band offset ratio $r \equiv \Delta E_C/\Delta E_V$ is found to be 60.4:39.6 (±2%), which agrees with the 60:40 rule.[8]

It is found that for samples with $x=0$ and 0.1, although ϕ_V can be readily measured both by BEES and s-BEES, ϕ_C cannot be measured due to the overwhelming internal hole current under the forward V_C needed for electron injection. For $x \geq 0.2$, the measured E_g of $Al_xGa_{1-x}As$ [Fig. 3(a)] agree well with the established values[7] (within 2%). In the direct-gap regime, no obvious band bowing effect was observed.[9] In the indirect-gap regime, E_g of L valley instead of the lower lying X valley in the CB is observed. This may be attributed to the short mean free path of X electrons in GaAs materials,[10] consistent with BEES results on direct-gap GaAs/$Al_xGa_{1-x}As$($x \leq 0.42$) SB HJs.[11]

The main results from the quaternary AlGaInP alloy are shown in Fig. 4. Figures 4(b) and 4(c) show the measured ϕ_V

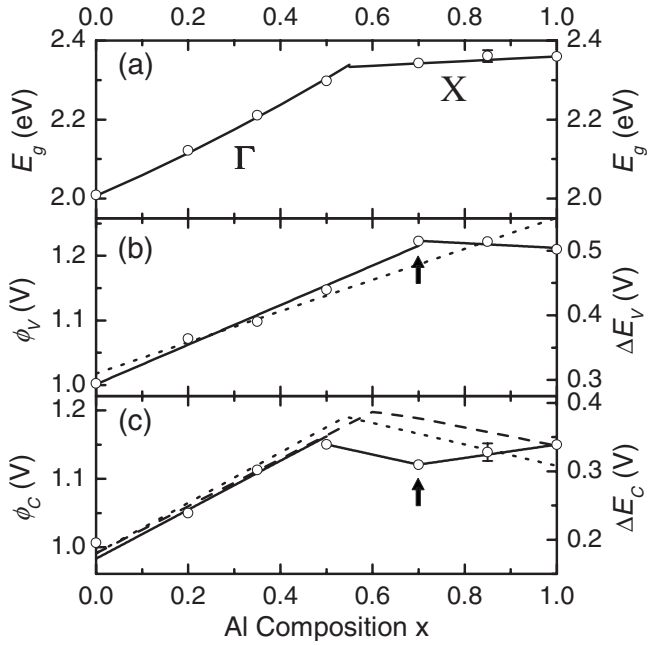

FIG. 4. Al composition x dependence of (a) E_g of $(Al_xGa_{1-x})_{0.51}In_{0.49}P$ (solid lines are from Ref. 7), (b) ϕ_V and ΔE_V of GaAs/$(Al_xGa_{1-x})_{0.51}In_{0.49}P$, and (c) ϕ_C and ΔE_C of GaAs/$(Al_xGa_{1-x})_{0.51}In_{0.49}P$. Dotted lines and dashed line are deduced from Refs. 12 and 13, respectively. Vertical arrows show the transition at $x \sim 0.7$.

and ϕ_C, as well as $\Delta E_V(x)$ and $\Delta E_C(x)$ derived the same way as above. $\Delta E_V(x)$ shows a linear dependence on x for $0<x<0.7$ as $\Delta E_V(x)=0.293+0.306x$ (eV) ($\pm 3\%$), which can be explained by an argument similar to the case for AlGaAs. For $x>0.7$, $\Delta E_V(x)$ decreases with x as $\Delta E_V(x)=0.541-0.037x$ ($\pm 4\%$). $\Delta E_C(x)$ shows a more complicated behavior. In the direct-gap regime ($0<x<0.5$), $\Delta E_C(x)$ increases linearly with x as $\Delta E_C=0.172+0.358x$ ($\pm 7\%$). The measured Γ band offsets agree well with the expected values deduced by the transitivity rule, i.e., adding $\Delta E_V=0.31$ eV and $\Delta E_C=0.18$ eV of the GaInP-GaAs HJ to the reported ΔE_V and ΔE_C on AlGaInP-GaInP HJs,[12,13] respectively. At $x>0.5$, ΔE_C starts to decrease signaling a direct-indirect transition of the CB minima. Surprisingly, ΔE_C increases with x again at $x>0.7$ as $\Delta E_C=0.242+0.097x$ ($\pm 1\%$). The measured E_g of $(Al_xGa_{1-x})_{0.51}In_{0.49}P$ [Fig. 4(a)] match well with the established values[7] (within 0.4%). The indirect E_g is found to be from the X valley in the CB. E_g does not show a transition at $x \sim 0.7$ because the opposite trends in the CB and the VB at $x>0.7$ are effectively canceled out. The Γ band offset ratio r for heteroanion GaAs/AlGaInP HJs increases from 37:63 at $x=0$ to 44:56 at $x=0.5$ ($\pm 8\%$). The band offsets tend to distribute more in the VB, as predicted by the common anion rule.[2]

It is intriguing that the observed indirect band offsets deviate from predictions by the transivity rule. Strain effects should be minimal since all the epilayers were grown at the same temperature and the AlGaInP layers are nearly lattice-matched (with $\leq 0.1\%$ compressive strain measured by x-ray diffraction) to the GaAs substrates. The ordering effect in AlGaInP alloys can be excluded because it would cause a lowering of the E_g,[14] which is not observed in our case. We tentatively attribute the breakdown of the transitivity rule as a result of the interfacial dipoles[15] formed at the polar GaAs/AlGaInP (100) interface, which awaits further investigation.

This work was supported by a DARPA HUNT Contract No. 222891-01 subaward from the University of Illinois at Urbana-Champaign, the NSF-funded Nanoscale Science and Engineering Center (NSEC), and the Center for Nanoscale Systems (CNS) at Harvard University.

[1] P. Y. Yu and M. Cardona, *Fundamentals of Semiconductors* (Springer, Berlin, 1996).
[2] E. T. Yu, J. O. McCaldin, and T. C. McGill, in *Solid State Physics*, edited by H. Ehrenreich and D. Turnbull (Academic, New York, 1992), Vol. 46.
[3] For recent reviews, see V. Narayanamurti and M. Kozhevnikov, Phys. Rep. **349**, 447 (2001); W. Yi, A. J. Stollenwerk, and V. Narayanamurti, Surf. Sci. Rep. **64**, 169 (2009).
[4] J. J. O'Shea, E. G. Brazel, M. E. Rubin, S. Bhargava, M. A. Chin, and V. Narayanamurti, Phys. Rev. B **56**, 2026 (1997).
[5] W. Yi, V. Narayanamurti, J. M. O. Zide, S. R. Bank, and A. C. Gossard, Phys. Rev. B **75**, 115333 (2007).
[6] L. D. Bell, M. H. Hecht, W. J. Kaiser, and L. C. Davis, Phys. Rev. Lett. **64**, 2679 (1990).
[7] I. Vurgaftman, J. R. Meyer, and L. R. Ram-Mohan, J. Appl. Phys. **89**, 5815 (2001).
[8] M. Missous, in *Properties of Aluminum Gallium Arsenide*, EMIS Datareviews Series No. 7, edited by S. Adachi (Inspec, London, 1993).
[9] G. Oelgart, R. Schwabe, M. Heider, and B. Jacobs, Semicond. Sci. Technol. **2**, 468 (1987).
[10] E. Y. Lee, S. Bhargava, M. A. Chin, and V. Narayanamurti, J. Vac. Sci. Technol. A **15**, 1351 (1997).
[11] M. Kozhevnikov, V. Narayanamurti, C. Zheng, Y.-J. Chiu, and D. L. Smith, Phys. Rev. Lett. **82**, 3677 (1999).
[12] F. A. Kish and R. M. Fletcher, in *High Brightness Light-Emitting Diodes*, Semiconductors and Semimetals, Vol. 48, edited by G. B. Stringfellow and M. G. Craford (Academic, San Diego, 1997).
[13] D. Vignaud and F. Mollot, J. Appl. Phys. **93**, 384 (2003).
[14] C. H. Chen, S. A. Stockman, M. J. Peanasky, and C. P. Kuo, in *High Brightness Light-Emitting Diodes*, Semiconductors and Semimetals, Vol. 48, edited by G. B. Stringfellow and M. G. Craford (Academic, San Diego, 1997).
[15] J. Tersoff, Phys. Rev. B **30**, 4874 (1984).